Progress in Oceanography 236 (2025) 103475

Contents lists available at ScienceDirect

Progress in Oceanography

journal homepage: www.elsevier.com/locate/pocean

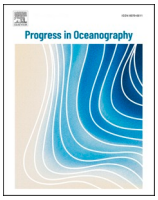

Kinorhyncha community in the Aleutian Trench (North Pacific Ocean) with the description of a new *Cristaphyes* species (Allomalorhagida, Pycnophyidae)☆

Nuria Sánchez [a,*], Frederic Bonk [b,c], Alberto González-Casarrubios [a]

[a] Complutense University of Madrid (UCM), Faculty of Biology, Department of Biodiversity, Ecology and Evolution (BEE), Madrid, Spain
[b] Deutsches Zentrum für Marine Biodiversitätsforschung, Senckenberg am Meer, Wilhelmshaven, Germany
[c] Institute of Biology and Environmental Sciences, Carl von Ossietzky, University Oldenburg, Germany

ARTICLE INFO

Keywords:
Kinorhynch
Taxonomy
Deep-sea
Hadal
Bering Sea
Diversity

ABSTRACT

Several species of trench-dwelling meiofaunal animals, including Kinorhyncha, have been described in recent years; however, our knowledge on kinorhynchs inhabiting abyssal and even hadal depths is still extremely scarce. In the present study, we explore the Kinorhyncha community of the Aleutian Trench, North Pacific Ocean, an under-sampled region in terms of meiofauna. As a result, a new species of *Cristaphyes* inhabiting abyssal and hadal depths of the trench is described. *Cristaphyes unangax* sp. nov. is characterized by the presence of middorsal processes on segments 1 – 10, with the last one extending well-beyond the posterior margin of the trunk. *Cristaphyes unangax* sp. nov. thus becomes the fourth hadal species described within the phylum Kinorhyncha. In terms of biodiversity, abundance of adult kinorhynchs remains relatively low along the trench's depth gradient (c.a. 3.500 – 7.200 m), except at two sites: one at the axis and another at the slope. The higher abundance at the axis aligns with patterns in other trenches, where organic matter accumulation enhances microbial activity, supporting meiofaunal communities. The elevated specimens at the slope station, located at abyssal depth, may result from Aleutian upwelling currents or trench terraces that facilitate food deposition. The Kinorhyncha community in the Aleutian Trench is dominated by *Echinoderes ultraabyssalis* and includes another nine species, many shared with the North Pacific and Arctic. These findings suggest that meiofauna in the North Pacific can disperse across bathymetric barriers, potentially linking the Aleutian and Kuril-Kamchatka trenches. Additionally, the Aleutian Trench may serve as a migration corridor for meiofauna between the North Pacific and Arctic, aided by strong bottom currents.

Zoobank: urn:lsid:zoobank.org:pub:56D1BA0B-3D9F-4547-84BC-C9BAFCA1D220

1. Introduction

Life in the deepest regions of the oceans is still largely unknown. The extreme conditions of pressure and darkness of deep-sea environments present significant challenges to studying and fully understanding the diversity of species that inhabit these regions. While numerous meiofaunal species, including members of the phylum Kinorhyncha, have been described in recent years, our knowledge on their diversity at abyssal and hadal depths remains severely constrained. For instance, only three hadal-dwelling species have been described up to date: *Echinoderes ultraabyssalis* Adrianov & Maiorova, 2019, from the Kuril-Kamchatka Trench; *Echinoderes mamaqucha* Grzelak et al., 2021, from the Atacama Trench; and *Echinoderes australis* Sánchez et al., 2024 (see Adrianov & Maiorova, 2019; Grzelak et al., 2021; Sánchez et al., 2024). Another finding drawn from investigations of the deep-sea kinorhynch community is that non-pycnophyid species are generally more prevalent in these environments than representatives of the family Pycnophyidae (Adrianov & Maiorova, 2015, 2019; Grzelak & Sørensen, 2019; Sørensen et al., 2018; Yamasaki et al., 2018a, 2018b, 2019; Sánchez et al., 2014, 2019, 2022, 2024; Cepeda et al., 2020; Grzelak et al., 2021). Despite this, when pycnophyids are found below 500 m depth (criterion for deep-sea species according to World Register of Deep-Sea Species, Glover et al., 2025), they are often representatives of *Cristaphyes*, which holds the highest number of deep-sea species within the family (four

☆ This article is part of a special issue entitled: 'AleutBio' published in Progress in Oceanography.

* Corresponding author.
E-mail address: nurisanc@ucm.es (N. Sánchez).

https://doi.org/10.1016/j.pocean.2025.103475

Available online 19 April 2025

species) with an average depth of occurrence exceeding 600 m (Glover et al., 2025). Notably, some species, such as *C. abyssorum* (Adrianov & Maiorova, 2015) and *C. nubilis* (Sánchez et al., 2014), have been documented even in abyssal zones at depths exceeding 4.000 m.

The genus *Cristaphyes* Sánchez et al., 2016, was established to encompass a group of allomalorhagid (formerly homalorhagid) kinorhynchs characterised by the presence of distinctive structures in middorsal position, designated as "middorsal processes" (Sánchez et al., 2016). These structures are cuticular protrusions extending beyond the posterior margins of the segments. Middorsal processes are typically present in specimens of *Cristaphyes* on segments 2 – 9, and often on segments 1 and 10 as well (Sánchez et al., 2016). Currently, the genus includes 25 species, making it the most species-rich genus within the family Pycnophyidae, alongside the type genus, *Pycnophyes* Zelinka, 1907.

Cristaphyes represents a group undergoing significant taxonomic development. Since its establishment in 2016, nine species have been described within this genus. This growth contrasts sharply with genera such as *Higginsium* Sánchez et al., 2016 or *Krakenella* Sánchez et al., 2016, which have seen few or no new species described since their elevation to generic status (Sánchez et al., 2016).

The aim of this contribution is to describe a new species of the genus *Cristaphyes* from the Aleutian Trench and nearby localities in the North Pacific Ocean. The Aleutian Trench is a prominent oceanic depression located in the Bering Sea, in the northernmost part of the Pacific Ocean. The trench extends approximately 3.200 km and reaches depths of up to 8.100 m (Lemenkova, 2021). To date, meiofaunal records from this vast area are limited to a single box core collected at the axis of the trench (Jumars & Hessler, 1976) together with still unpublished data from 150 stations sampled during the SO249 deep-sea expedition (Werner et al., 2016). This work, therefore, represents the first description of an animal species from this benthic community.

2. Material and methods

2.1. Sampling and processing

Sediment samples were collected using a multicorer (9.4 cm inner diameter) between 27th July and 30th August 2022 as part of the Aleut Bio (Aleutian Trench Biodiversity Studies, SO293) expedition aboard the research vessel Sonne (Brandt, 2022). Sampling stations were located in the northeastern Pacific, encompassing the Bering Sea, adjacent areas of the Aleutian Trench, and the trench itself (Fig. 1). Detailed information from each sampling site and the kinorhynch fauna of each site is provided in Table 1.

The upper 5 cm of the sediment cores were preserved in 4 % formalin. The samples were then centrifuged three times in a Kaolin/Levasil solution at 4.000 rpm for 6 min per cycle, following the protocol described by Neuhaus & Blasche (2006), and subsequently sieved using a 40 μm mesh.

2.2. Morphological observation

Kinorhyncha specimens were sorted under a stereomicroscope. For light microscopy, the specimens were dehydrated through a graded series of ethanol and glycerine and then maintained in 100 % glycerine for 24 h. Subsequently, the specimens were mounted on glass slides using dimethyl hydantoin formaldehyde resin (DMHF). Identification and morphological descriptions were conducted using an Olympus© BX51 microscope equipped with differential interference contrast optics and an Olympus© DP70 camera.

For scanning electron microscopy (SEM), adult specimens underwent a dehydration process through a graded series of ethanol and acetone, followed by critical-point drying. The dried specimens were mounted on stubs, sputter-coated with gold, and examined using a JEOL© Ltd. JSM-6335F at the National Centre for Electron Microscopy (CNME), Complutense University of Madrid.

Identification to the genus level was performed using the taxonomic keys provided by Sánchez et al. (2016). Taxonomic measurements followed the procedures outlined by González-Casarrubios et al. (2023), incorporating an additional measurement of a morphological structure: the keel-shaped and/or spinose middorsal processes. Accurately measuring these structures along their entire length is challenging, as their point of origin is often not clearly visible. To minimize errors, only the free portion of the processes should be considered. Therefore, measurements should be taken from the distal end to the posterior area of the segment, specifically up to the end of the free flap. Measurements of the new species are included in the supplementary materials of this study (Supplementary Material 1) and are also accessible in the Kinorhyncha Measurement Database (González-Casarrubios & Yamasaki, 2022).

Line art illustrations and image compositions were created using Adobe® Photoshop and Illustrator 2022 software. Type and non-type material of the new species was deposited at the Museum für

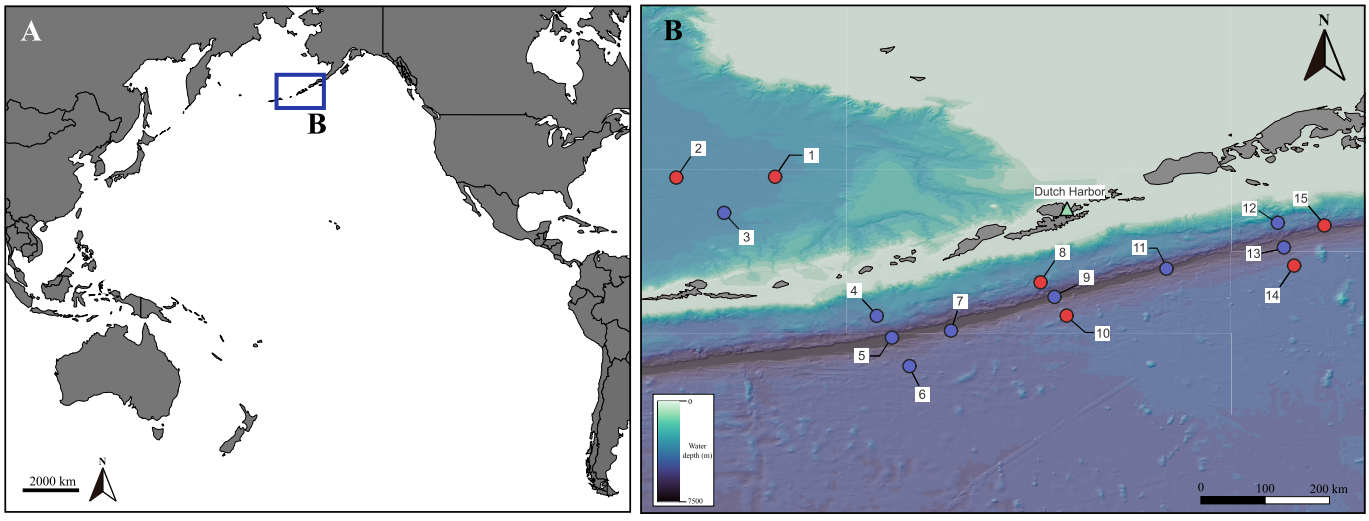

Fig. 1. Map showing the collection area of the new species. A. General map indicating the specific location of the sampling area. B. Close-up of the sampling area. The dots represent sampling stations, with numbered red dots indicating the stations where specimens of the new species were found. (For interpretation of the references to colour in this figure legend, the reader is referred to the web version of this article.)

Table 1
Summary of data on stations where specimens of the new species were found. The associated kinorhynch fauna is included as well as the species found in other stations sampled during the Aleut Bio cruise. Digits in parentheses refer to the number of specimens. Catalogue numbers in bold refer to holotype.

Station	Deployment	Date	Lat N	Long W	Depth (m)	Mounting	Catalogue number and n. of specimens
1	7	27.07.2022	54°33.213′	172°34.949′	3510	LM	*Cristaphyes unangax* sp. nov. (3♂) ZMB 12968–12970
1	8	27.07.2022	54°33.221′	172°34.951′	3511	LM	*Cristaphyes unangax* sp. nov. (1♂) ZMB 12971
2	8	29.07.2022	54°32.214′	174°37.634′	3653	LM	*Cristaphyes unangax* sp. nov. (1♂, 1♀) ZMB 12972, 12973
4	7	02.08.2022	51°40.336′	170°28.698′	4642	LM	*Echinoderes juliae* Sørensen et al., 2018 (1) ZMB 12982
						LM	*Condyloderes kurilensis* Adrianov & Maiorova, 2016 (1) ZMB 12983
4	8	02.08.2022	51°40.332′	170°28.702′	4642	LM	*Sphenoderes japonicus* Adrianov & Maiorova, 2024 (1) ZMB 12984
5	6	04.08.2022	51°13.312′	170°09.847′	7237	LM	*Echinoderes ultraabyssalis* Adrianov & Maiorova, 2019 (1) ZMB 12895
6	6	07.08.2022	50°37.933′	169°48.076′	5316	LM	*Cristaphyes unangax* sp. nov. (1♂, 1♀) ZMB 12974, 12075
						LM	*Echinoderes juliae* Sørensen et al., 2018 (1) ZMB 12986
6	7	07.08.2022	50°37.928′	169°48.079′	5317	LM	*Cristaphyes unangax* sp. nov. (1♀) ZMB 12976
						SEM	*Cristaphyes unangax* sp. nov. (1♀) ZMB 12977
7	6	10.08.2022	51°22.003′	168°56.567′	6557	LM	*Sphenoderes japonicus* Adrianov & Maiorova, 2024 (1) ZMB 12987
8	6	13.08.2022	52°21.968′	167°05.275′	4612	LM	*Cristaphyes unangax* sp. nov. (1♂) ZMB 12978
						LM	*Condyloderes kurilensis* Adrianov & Maiorova, 2016 (1) ZMB 12988
8	7	13.08.2022	52°21.983′	167°05.277′	4612	SEM	*Cristaphyes unangax* sp. nov. (1) ZMB 12977
						LM	*Echinoderes ultraabyssalis* Adrianov & Maiorova, 2019 (1) ZMB 12989
						LM	*Cephalorhyncha polunga* (1) ZMB 12990
9	5	15.08.2022	52°03.914′	166°48.041′	7137	LM	*Echinoderes ultraabyssalis* Adrianov & Maiorova, 2019 (1) ZMB 12991
9	9	16.08.2022	52°09.090′	166°57.525′	6472	LM	*Echinoderes ultraabyssalis* Adrianov & Maiorova, 2019 (3) ZMB 12992–12994
9	10	16.08.2022	52°09.103′	166°57.521′	6469	LM	*Echinoderes ultraabyssalis* Adrianov & Maiorova, 2019 (12) ZMB 12995–13006
10	7	19.08.2022	51°40.609′	166°32.964′	5097	LM	*Cristaphyes unangax* sp. nov. (1♂) ZMB 12979
						LM	*Echinoderes delaordeni* Sánchez et al., 2022 (1) ZMB 13007
12	7	24.08.2022	53°36.028′	162°10.664′	4305	LM	*Echinoderes angustus* Higgins & Kristensen, 1988 (2) ZMB 13008, 13009
						LM	*Echinoderes ultraabyssalis* Adrianov & Maiorova, 2019 (8) ZMB 13010–13017
						LM	*Echinoderes* unidentified (1) ZMB 12318
12	8	24.08.2022	53°36.028′	162°10.664′	4303	LM	*Echinoderes angustus* Higgins & Kristensen, 1988 (1) ZMB 13019
						LM	*Echinoderes hamiltonorum* (1) ZMB 13020
						LM	*Echinoderes ultraabyssalis* Adrianov & Maiorova, 2019 (3) ZMB 13021–13023
						LM	*Cephalorhyncha polunga* (1) ZMB 13024
						LM	*Sphenoderes japonicus* Adrianov & Maiorova, 2024 (1) ZMB 13025
						LM	Semnoderidae (1) ZMB 13026
13	5	26.08.2022	53°05.374′	162°03.156′	6430	LM	*Echinoderes ultraabyssalis* Adrianov & Maiorova, 2019 (3) ZMB 13027–13029
						LM	*Sphenoderes japonicus* Adrianov & Maiorova, 2024 (1) ZMB 13030
13	6	26.08.2022	53°05.348′	162°03.170′	6341	LM	*Echinoderes ultraabyssalis* Adrianov & Maiorova, 2019 (1) ZMB 13031
						LM	*Condyloderes kurilensis* Adrianov & Maiorova, 2016 (3) ZMB 13032–13034
						LM	*Centroderes* sp.1 (1) ZMB 13035
14	7	28.08.2022	52°42.809′	161°50.484′	4871	LM	*Cristaphyes unangax* sp. nov. (2♂, 1♀) **ZMB 12965**♂, 12966♂, 12967♀
15	4	30.08.2022	53°32.686′	161°12.855′	6265	LM	*Cristaphyes unangax* sp. nov. (2♀) ZMB 12980, 12981
						LM	*Condyloderes kurilensis* Adrianov & Maiorova, 2016 (1) ZMB 13036

Naturkunde of Berlin (MfN).

3. Results

3.1. Taxonomic account

Order Allomalorhagida (Sørensen et al., 2015) *sensu* Herranz et al., 2022.

Family Pycnophyidae Zelinka, 1896.

Genus *Cristaphyes* Sánchez et al., 2016.

Cristaphyes unangax sp. nov.

(Figs. 2 – 4; Tables 2 – 3).

urn:lsid:zoobank.org:pub:56D1BA0B-3D9F-4547-84BC-C9BAFCA1D220.

3.2. Material examined

Type material: collected on 27/07/2022 to 30/08/2022 at Aleutian Trench, North Pacific Ocean. Holotype, adult male: Station 14(7); Coordinates 52°42.809 N, 161°50.484 W; at 4.871 m depth; mounted in DMHF, deposited at Museum für Naturkunde Berlin (MfN), collection "Vermes", Generalkatalog Free-living Worms, under catalogue number: ZMB – 12965. Paratypes, 15 adult specimens, 10 males and 5 females, deposited at MfN under catalogue numbers: ZMB 12966–12976 and ZMB 12978–12981. Detailed information from each sampling site is provided in Table 1.

Non-type material: 2 adult specimens: 1 adult, indeterminate sex (Station 8); mounted for SEM examination, deposited at MfN under catalogue number: ZMB 13067; 1 adult female (Station 6); mounted for SEM examination, deposited at MfN under catalogue number: ZMB 12977. Detailed information from each sampling site is provided in Table 1.

Type locality: Aleutian Trench, North Pacific Ocean, 52°42.809 N, 161°50.484 W, 4.871 m depth.

3.3. Etymology

The specific name, *unangax*, refers to the Unangax̂ communities, currently known as the Aleut, the native people of Alaska who inhabited the Aleutian Islands prior to the arrival of Russian explorers.

3.4. Diagnosis

Cristaphyes with keel-shaped middorsal processes on segments 1 – 10,

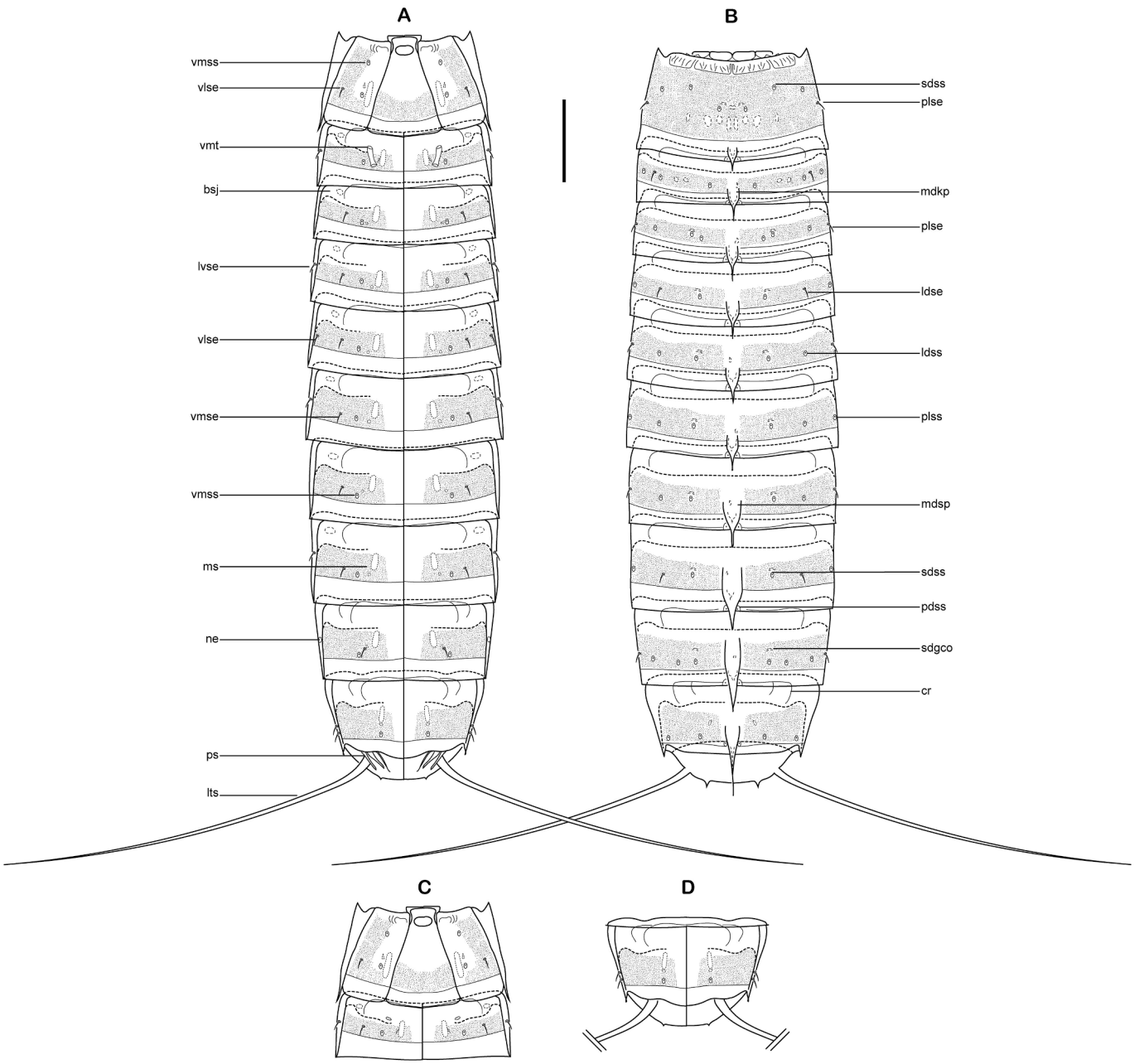

Fig. 2. Line art illustrations of adult *Cristaphyes unangax* sp. nov. A: Male in ventral view; B: Male in dorsal view; C: Female segments 1–2 in ventral view; D: Female segments 10–11 in ventral view. Scale: 100 μm. Abbreviations: bsj, ball-and-socket joint; cr, cuticular ridge; ldse, laterodorsal seta; ldss, laterodorsal sensory spot; lts, lateral terminal spine; lvse, lateroventral seta; mdkp, middorsal keel-shaped process; mdsp, middorsal spinose process; ms, muscular scar; ne, nephridiopore; pdss, paradorsal sensory spot; plse, paralateral seta; plss, paralateral sensory spot; ps, penile spine; sdgco, subdorsal glandular cell outlet; sdss, subdorsal sensory spot; vlse, ventrolateral seta; vmse, ventromedial seta; vmss, ventromedial sensory spot; vmt, ventromedial tube.

slightly increasing in length towards the posterior segments; with those of segments 6 – 9 as spinose processes, more flexible, and with the process of segment 10 extending well-beyond the posterior margin of segment 11. Both sexes with lateroventral setae on segments 2, 4, 6, 8 and 10 (two pairs), and ventrolateral ones on segment 1 and 5; males with paired setae in paralateral positions on segments 1, 3, 5, 7 and 9, laterodorsal ones on segments 2, 4 and 8 (maybe also on 6 and 9), and ventromedial ones on segments 3 – 9; females with laterodorsal setae on segments 2 and 9, paralateral setae on segment 1, and ventromedial ones on segments 2, 7 – 9. Lateral terminal spines long, slender (LTS:TL males and females average ratio 29 %).

3.5. Description

See Table 2 for measurements and Table 3 for locations of middorsal cuticular specializations, setae, tubes and sensory spots.

Head. With retractable mouth cone and introvert, which are retracted inside the trunk in the observed specimens, hence details on the morphology and distribution of oral styles and scalids cannot be provided.

Neck. Four dorsal and two ventral placids (Fig. 2B, 3A). Dorsal placids equal in size, rectangular, robust and concave (ca. 28–35 μm wide and 8–17 μm high) (Fig. 3A); ventral ones equal in size rectangular, robust and concave (ca. 30–38 μm wide and 8–13 μm high).

Trunk. With 11 segments (Fig. 2A–B, 4A). Segment 1 with one tergal,

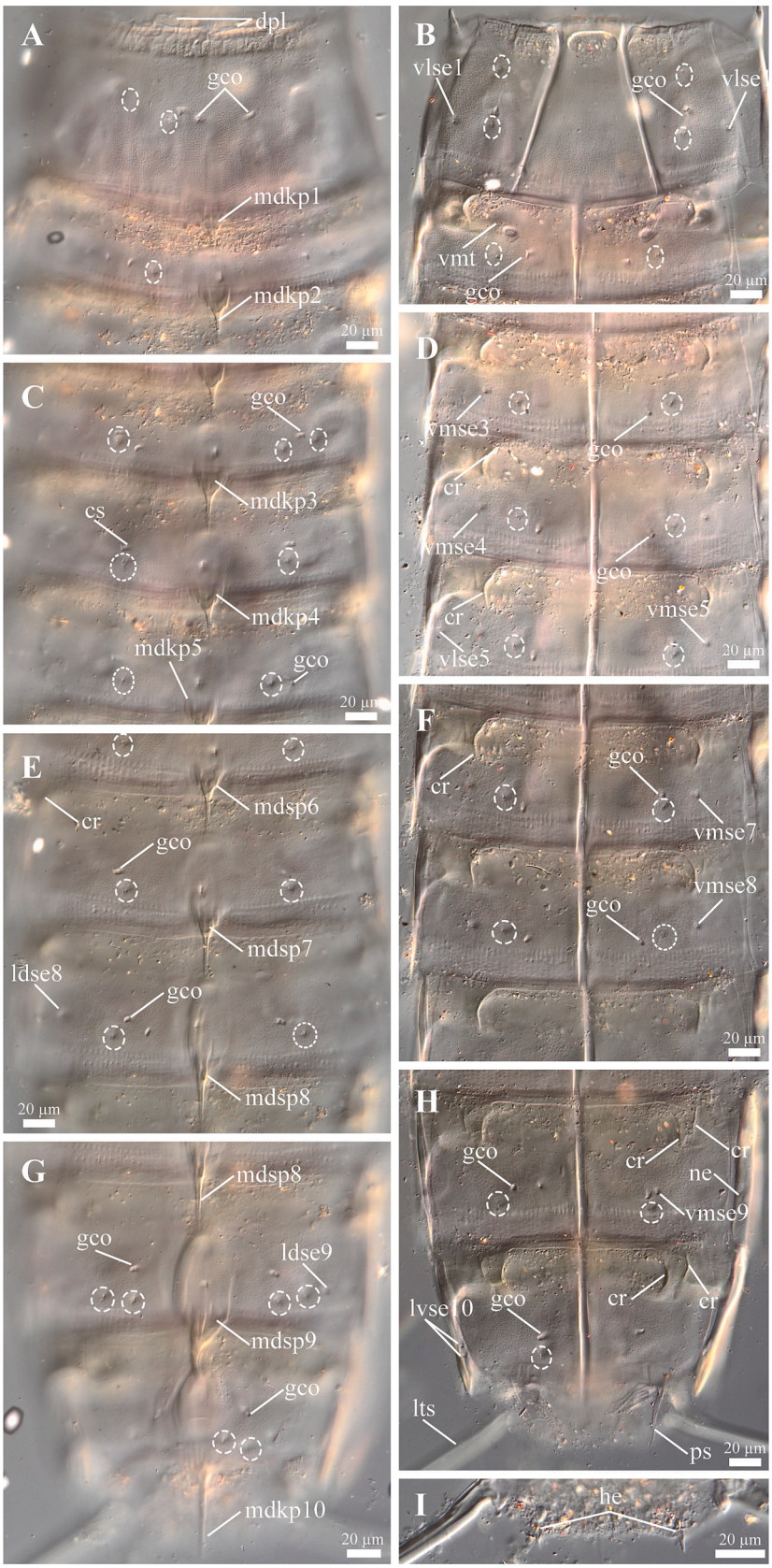

(caption on next page)

Fig. 3. Light micrographs of male holotype of *Cristaphyes unangax* sp. nov., showing details on the neck and segments 1–11. A: Dorsal view on the neck and segments 1–2; B: Ventral view of segments 1–2; C: Dorsal view on segments 3–5; D: Ventral view on segments 3–5; E: Dorsal view on segments 6–8; F: Ventral view on segments 6–8; G: Dorsal view on segments 9–11; H: Ventral view on segments 9–11; I: Ventral view on segment 11. Abbreviations: cr, cuticular ridge; dpl, dorsal placid; gco, glandular cell outlet; he, horn-shaped extension; ldse, laterodorsal seta; lts, lateral terminal spine; lvse, lateroventral seta; mdkp, middorsal keel-shaped process; mdsp, middorsal spinose process; ne, nephridiopore; ps, penile spine; vlse, ventrolateral seta; vmse, ventromedial seta; vmt, ventromedial tube; numbers after abbreviations indicate corresponding segment; sensory spots are marked as dashed circles.

two episternal and one trapezoidal, midsternal plate (Fig. 3B, 4B); remaining segments with one tergal and two sternal cuticular plates. Sternal cuticular plates relatively narrow, almost constant in width along the trunk and tapering at the last trunk segments, maximum width of sternal plates at segment 6 (MSW-6:TL average ratio = 23 %). Middorsal processes on segments 1 – 10, pointed, projecting beyond the posterior margin of segments, progressively longer and turning more spinose towards the posterior segments, reaching their maximum length on segment 9 or 10 and with that of segment 10 extending well-beyond the posterior margin of segment 11 (Fig. 2B, 4A). Middorsal process covered by short, thick cuticular hairs (Fig. 4F). Dorsal glandular cell outlets as rounded to oval subdorsal perforations on segments 2 – 9 (Fig. 3C, E, G), and in paradorsal position on segments 1 and 10 (Fig. 3A, G), also present at the base of the middorsal processes. Ventral glandular cell outlets as rounded to oval ventromedial perforations on segments 2 – 10 (Fig. 3B, D, F, H), and as crescentic ventromedial perforations on segment 1 (Fig. 3B). One pair of cuticular ridges in laterodorsal position on segments 2 – 10 (Fig. 2B, 3E, G, 4C), plus one pair in subdorsal position on segments 9 – 10. One pair of ventrolateral cuticular ridges on segments 2 – 10 (Fig. 2A, 3D, F, H, 4K), plus an extra pair in ventromedial position on segments 9 and 10 (Fig. 3H, 4K). Minute glandular cell outlets may be present adjacent to cuticular ridges (Fig. 4K). Pachycycli and ball-and-socket joints conspicuous on segments 2 – 8, reduced on most posterior segments (Fig. 2). Apodemes absent. Primary pectinate fringes finely serrated (Fig. 4E); secondary pectinate fringes as a wavy, quite inconspicuous single line in laterodorsal and ventrolateral positions at the anterior most region of the segments (Fig. 4C–D). Muscular scars as rounded to oval areas in laterodorsal (very inconspicuous) and ventromedial positions on segments 1 – 10 (Fig. 2A).

Segment 1. Anterolateral margins of the tergal plate with horn-like extensions (Fig. 4A). Anterior edge of tergal plate denticulated, with cuticular wrinkles forming a net-like ornamentation across the anterior margin of the plate (Fig. 2B, 3A, 4A). Anterior margin of ventral plates with ridges forming a quadrangular depression on each episternal plate; and a large rectangular depression on the midsternal plate (Fig. 2A, 3B). Trapezoidal midsternal plate, wider at the base (ca. 34 – 38 μm wide at the most anterior margin, ca. 84 – 87 μm wide at the most posterior margin; average ratio = 42 %), with straight lateral margins. Keel-shaped middorsal process surpassing the posterior margin of the segment (Fig. 2B, 3A, 4A). Paired setae in paralateral and ventrolateral positions (Fig. 2A–B, 3B, 4G). Sensory spots on this and following segments as oval areas with cuticular micropapillae surrounding one or two pores (Fig. 4J). Sensory spots in paradorsal (in the basal part of the middorsal process, near the posterior margin), subdorsal (two pairs), laterodorsal and ventromedial (two pairs) positions (Fig. 2A–B, 3A–B, 4B).

Segment 2. Keel-shaped middorsal process slightly longer than that of the preceding segment (Fig. 2B, 3A, 4A). Paired setae in laterodorsal and lateroventral positions (Fig. 2A–B). Females with a pair of setae in ventromedial position (Fig. 4B); males with tubes in ventromedial position (Fig. 3B). Sensory spots in paradorsal, subdorsal, laterodorsal, paralateral and ventromedial positions (Fig. 3A–B, 4B). Two pairs of subdorsal glandular cell outlets (Fig. 2B).

Segment 3. Keel-shaped middorsal process slightly longer than that of the preceding segment (Fig. 2B, 3C, 4A, C, E–F). Only males with paired setae in paralateral and ventromedial positions (Fig. 2A–B, 3D). Sensory spots in paradorsal, subdorsal (two pairs), laterodorsal and ventromedial positions, the latter more mesial than the ventromedial setae (Fig. 3C–D, 4B–C, F).

Segment 4. Keel-shaped middorsal process slightly longer than that of the preceding segment (Fig. 2B, 3C, 4A, E). Paired lateroventral setae (Fig. 2A). Only males with paired setae in laterodorsal and ventromedial positions (Fig. 2A–B, 3C–D, 4B). Sensory spots in paradorsal, subdorsal, paralateral and ventromedial positions, the latter more mesial than the ventromedial setae (Fig. 2A–B, 3C–D, 4E).

Segment 5. Keel-shaped middorsal process slightly longer than that of the preceding segment (Fig. 2B, 3C, E, 4A, E). Paired ventrolateral setae (Fig. 4D). Only males with paired setae in paralateral and ventromedial positions (Fig. 2B, 3D, 4D). Sensory spots in paradorsal, subdorsal, laterodorsal and ventromedial positions, the latter more mesial than the ventromedial setae (Fig. 3C–D).

Segment 6. Spinose middorsal process, with flexible distal end, slightly longer than that of the preceding segment (Fig. 2B, 3E, 4A). Paired lateroventral setae (Fig. 2A). Only males with paired setae in ventromedial positions (Fig. 2A–B, 3F, 4D). Sensory spots in paradorsal, subdorsal, laterodorsal, paralateral and ventromedial positions, the latter more mesial than the ventromedial setae (Fig. 2A–B, 3E–F, 4D).

Segment 7. Spinose middorsal process, with flexible distal end, slightly longer than that of the preceding segment (Fig. 2B, 3E, 4A). Paired ventromedial setae (Fig. 2A, 3F). Only males with paired setae in paralateral positions (Fig. 2A–B, 3F). Sensory spots in paradorsal, subdorsal, laterodorsal and ventromedial positions, the latter more mesial than the ventromedial setae (Fig. 2A–B, 3E–F, 4D).

Segment 8. Spinose middorsal process, with flexible distal end, longer than that of the preceding segment (Fig. 2B, 3G, 4A, I). Paired lateroventral and ventromedial setae (Fig. 2A, 3F, 4H). Only males with paired setae in laterodorsal positions (Fig. 2A–B, 3E–F). Sensory spots in paradorsal, subdorsal, paralateral and ventromedial positions, the latter more mesial than the ventromedial setae (Fig. 2A–B, 3E–F, 4H–J).

Segment 9. Spinose middorsal process, with flexible distal end, longer than that of the preceding segment (Fig. 2B, 3G, 4A, I, L). Paired ventromedial setae (Fig. 2A, 3H, 4H). Only males with paired setae in paralateral positions (Fig. 2A). Females with laterodorsal setae (Fig. 4M). Sensory spots in paradorsal, subdorsal (two pairs), laterodorsal and ventromedial positions, the latter more mesial than the ventromedial setae (Fig. 2A–B, 3G–H, 4H–I, L–M). Nephridiopore as small opening surrounded by short tubes in lateroventral position (Fig. 3H).

Segment 10. Keel-shaped middorsal process, more rigid than the spinose process of previous segments, commonly slightly longer than the spinose middorsal process of the preceding segment, twice as long as the keel-shaped of the anterior trunk segments (MDP5/MDP10 = 62 %, see Table 2) and extending well-beyond the posterior margin of segment 11 (Fig. 2B, 3G, 4A, I, K). Two pairs of setae in lateroventral positions (Fig. 3H). Sensory spots in paradorsal, subdorsal, laterodorsal and ventromedial positions (Fig. 2A–B, 3G–H, 4K). Tergal plate with slightly rounded posterior margin; sternal plates distally straight in females (Fig. 4K), more pointed in males (Fig. 3H).

Segment 11. Without middorsal cuticular specialization (Fig. 2B). Tergal pate with conspicuous horn-shaped extensions (Fig. 3I, 4K). Males with two pairs of stout, thick penile spines and one pair of penile bristles (Fig. 3H). Large lateral terminal spines (Fig. 2A–B, 3H, 4A, K) of similar size in both sexes (males LTS:TL average ratio 29 %; females LTS:TL average ratio 31 %).

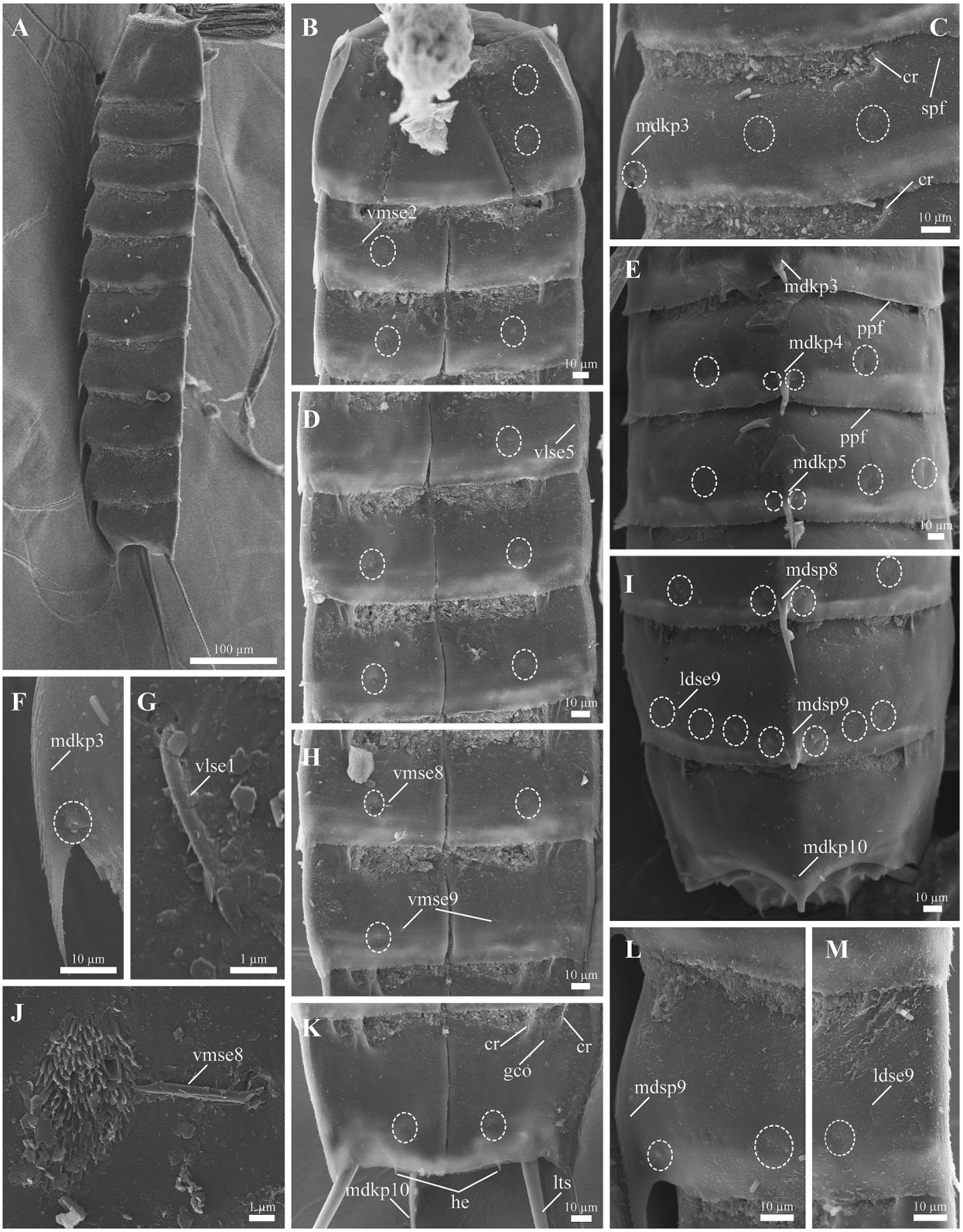

Fig. 4. Scanning electron micrographs of two additional specimens of *Cristaphyes unangax* sp. nov., showing trunk overview and cuticular details of the trunk segments. Female specimen (A–D, F–H, J–M); specimen of indeterminate sex (E, I). A: Lateral trunk overview; B: Ventral view of segments 1–3; C: Right side of the tergal plate of segment 3; D: Ventral view on segments 5–7; E: Dorsal view on segments 4–5; F: Detail of the middorsal process of segment 3; G: Detail of ventrolateral seta of segment 1; H: Ventral view on segments 8–9; I: Dorsal view on segments 8–11 (middorsal processes of segments 9 and 10 are broken); J: Detail of the ventromedial sensory spot and seta of segment 8; K: Ventral view on segment 10; L: Detail of the middorsal process of segment 9; M: Detail of the lateral region of segment 9. Abbreviations: cr, cuticular ridge; gco, glandular cell outlet; he, horn-shaped extension; ldse, laterodorsal seta; lts, lateral terminal spine; mdkp, middorsal keel-shaped process; mdsp, middorsal spinose process; ppf, primary pectinate fringe; spf, secondary pectinate fringe; vlse, ventrolateral seta; vmse, ventromedial seta; numbers after abbreviations indicate corresponding segment; sensory spots are marked as dashed circles.

Table 2
Measurements (μm) of the holotype (ZMB 12965) and type series of *Cristaphyes unangax* sp. nov. Numbers in the first column indicate the corresponding segment. Abbreviations: CL, cumulative length; LTS, lateral terminal spine; MDKP, middorsal keel-shaped process; MDSP, middorsal spinose process; MSW, maximum sternal width, measured on segment 6; n, number of measured specimens; S, segment length; SD, standard deviation; SW, standard width, measured on segment 10; TL, total trunk length.

Character	Holotype♂	n	Mean ♀	Range ♀	Mean ♂	Range ♂	Mean ♂♀	Range ♂♀	SD ♂♀
TL	912	8♂/3♀	856	838 – 881	842	804 – 912	846	804 – 912	31,34
CL	989	8♂/3♀	960	936 – 1050	969	880 – 1012	974	880 – 1050	47,29
CL/TL (%)	108	8♂/3♀	112	105 – 119	115	106 – 124	115	106 – 124	5,79
MSW6	210	6♂/3♀	184	163 – 295	196	186 – 210	192	163 – 210	13,22
MSW6/TL (%)	23.02	6♂/3♀	22	19 – 21	23	22 – 26	23	19 – 26	0,02
SW10	190	7♂/3♀	172	164 – 177	166	147 – 190	168	147 – 190	13,22
SW10/TL (%)	21	7♂/3♀	20	19 – 21	20	18 – 22	20	18 – 22	0,02
S1	120	8♂/3♀	122	114 – 126	119	111 – 129	120	111 – 129	5,27
S2	81	8♂/3♀	78	75 – 82	76	71 – 81	77	71 – 82	3,72
S3	80	8♂/3♀	80	73 – 89	79	71 – 83	79	71 – 89	5,38
S4	87	8♂/3♀	84	77 – 92	85	80 – 89	85	77 – 92	4,27
S5	87	8♂/3♀	86	78 – 99	89	83 – 94	88	78 – 99	6,34
S6	98	8♂/3♀	94	87 –105	97	79 – 108	96	79 – 108	8,48
S7	93	8♂/3♀	95	88 – 102	94	85 – 102	95	85 – 102	5,77
S8	94	7♂/3♀	99	94 – 104	97	93 – 101	98	93 – 104	3,71
S9	97	8♂/3♀	101	100 – 103	96	88 – 102	97	88 – 103	5,24
S10	94	8♂/3♀	98	91 – 103	97	93 – 102	97	91 – 103	3,98
S11	58	8♂/3♀	52	48 – 57	51	42 – 58	52	42 – 58	5,01
MDKP5	25	8♂/3♀	20	16 – 24	25	23 – 28	24	16 – 28	3,26
MDSP6	25	8♂/2♀	25	21 – 28	26	21 – 29	25	21 – 29	2,95
MDSP7	23	8♂/3♀	23	18 –28	27	23 – 32	26	18 – 32	3,97
MDSP8	29	8♂/3♀	30	27 – 32	31	27 – 38	31	27 – 38	3,43
MDSP9	41	7♂/3♀	41	34 – 46	37	30 – 49	38	30 – 49	6,53
MDSP10	49	6♂/2♀	52	40 – 63	44	28 – 72	46	28 – 72	15,88
LTS	241	5♂/3♀	259	229 –277	249	225 – 281	253	225 – 281	22,5
LTS/TL (%)	26	5♂/3♀	30	27 – 33	29	26 – 32	30	26 – 33	2,59

Table 3
Summary of nature and arrangement of setae, tubes, glandular cell outlet, sensory spots and nephridiopore in adults of *Cristaphyes unangax* sp. nov.; ♀, arrangement of character of females; ♂, arrangement of character of males. Abbreviations: kp, keel-shaped process; LD, laterodorsal; lts, lateral terminal spines; LV, lateroventral; MD, middorsal; ne, nephridiopore; PD, paradorsal; PL, paralateral; ps, penile spine; se, seta; SD, subdorsal; sp, spinose process; ss, sensory spot; tu, tube; VL, ventrolateral; VM, ventromedial.

Segment	MD	PD	SD	LD	PL	LV	VL	VM
♂								
1	kp	ss	ss, ss	ss	se		se	ss, ss
2	kp	ss	ss	ss, se	ss	se		ss, tu
3	kp	ss	ss, ss	ss	se			se, ss
4	kp	ss	ss	se	ss	se		se, ss
5	kp	ss	ss	ss	se		se	se, ss
6	sp	ss	ss	ss	ss	se		se, ss
7	sp	ss	ss	ss	se			se, ss
8	sp	ss	ss	se	ss	se		se, ss
9	sp	ss	ss, ss	ss	se	ne		ss, se
10	kp	ss	ss	ss		se(x2)		ss
11				ps(x3)		lts		
♀								
1	kp	ss	ss, ss	ss	se		se	ss, ss
2	kp	ss	ss	ss	ss	se		ss, se
3	kp	ss	ss, ss	ss				ss
4	kp	ss	ss		ss	se		ss
5	kp	ss	ss	ss			se	ss
6	sp	ss	ss	ss	ss	se		ss
7	sp	ss	ss	ss				se, ss
8	sp	ss	ss		ss	se		se, ss
9	sp	ss	ss, ss	ss		ne		ss, se
10	kp	ss	ss	ss		se(x2)		ss
11						lts		

3.6. Intraspecific variation

Segment 6. One female with a ventromedial seta in the right sternal plate. Laterodorsal setae instead of sensory spots present in three males, unpaired laterodorsal seta instead of sensory spot on the left side in one male.

Segment 8. One male without the laterodorsal seta of the left side.

Segment 9. Three males and one specimen of indeterminate sex with laterodorsal setae (Fig. 3G, 4I), one male with laterodorsal seta on the left side. Two males without paralateral setae. Three males with ventromedial setae laterally displaced, one male and one female with the right seta laterally displaced.

3.7. Kinorhyncha community in the Aleutian Trench

Nine species of Kinorhyncha were found at the abyssal depth of the study area: *Cephalorhyncha polunga* Sánchez et al., 2019; *Condyloderes kurilensis* Adrianov & Maiorova, 2016; *Cristaphyes unangax* sp. nov., *Echinoderes angustus* Higgins & Kristensen, 1988; *Echinoderes delaordeni* Sánchez et al., 2022; *Echinoderes hamiltonorum* Sørensen et al., 2018; *Echinoderes juliae* Sørensen et al., 2018; *Echinoderes ultraabyssalis*, and *Sphenoderes japonicus* Adrianov & Maiorova, 2024 (see Fig. 5). Of them, *Condyloderes kurilensis*, *Cristaphyes unangax* sp. nov., *Echinoderes ultraabyssalis* and *Sphenoderes japonicus* were also present at hadal depths of the trench, together with *Centroderes* sp.1 (see Fig. 5). In terms of abundance, *Echinoderes ultraabyssalis* was the dominant species at both bathyal ranges, with 12 and 21 specimens (see Fig. 5).

4. Discussion

4.1. Taxonomic remarks

Eight described species of *Cristaphyes* have lateral terminal spines and a keel-shaped process on segment 10 surpassing the posterior margin of the trunk, namely, *C. abyssorum*, *C. arctous* (Adrianov, 1999 in Adrianov & Malakhov, 1999), *C. chukchiensis* (Higgins, 1991), *C. cristatus* (Sánchez et al., 2013), *C. dordaidelosensis* Sørensen & Grzelak, 2018, *C. furugelmi* (Adrianov, 1999 in Adrianov & Malakhov, 1999), *C. glaurung* Sørensen & Grzelak, 2018, and *C. nubilis* (see Higgins, 1991; Adrianov & Malakhov, 1999; Sánchez et al., 2013, 2014; Adrianov & Maiorova, 2015; Sørensen & Grzelak, 2018). Out of these, *C. arctous* is

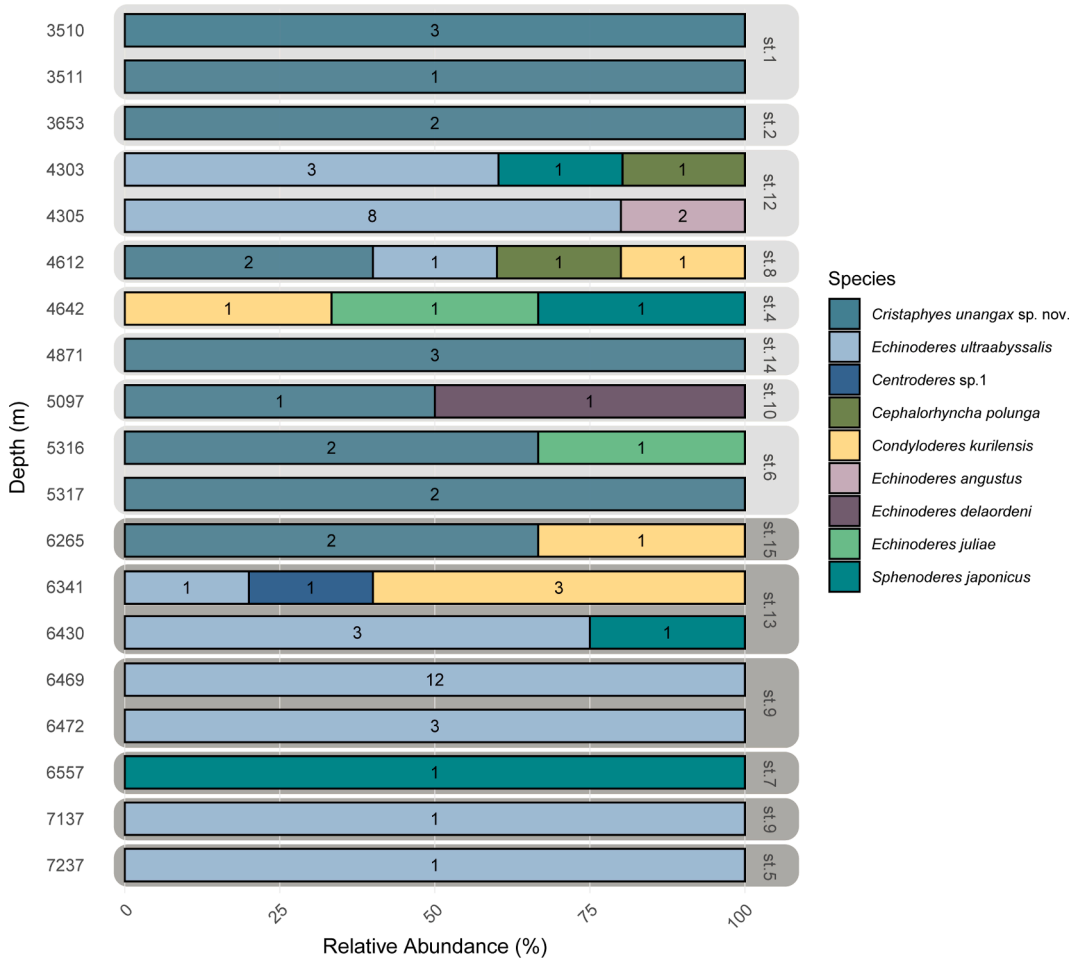

Fig. 5. Bathymetric distribution of Kinorhyncha community along the Aleutian Trench hadal (dark gray), abyssal zone (light gray), and adjacent abyssal plain (light gray). Bars show the relative abundance (%) of each species, digits on bars refer to the total abundance of each species, numbers after "st." refer to the station number.

easily distinguished from the new species by its obtuse and blunt middorsal processes on segments 1 – 7 (Adrianov & Malakhov, 1999), which differ from the conspicuously pointed ones observed in *C. unangax* sp. nov.

The remaining species differ from *Cristaphyes unangax* sp. nov. in the pattern of setae. *Cristaphyes abyssorum* only has lateroventral setae on segment 10 (females also on segment 1), *C. chukchiensis*, *C. dordaidelosensis* and *C. glaurung* have lateroventral setae on segments 2 – 10 (see Higgins, 1991; Adrianov & Maiorova, 2015; Sørensen & Grzelak, 2018), while *C. unangax* sp. nov. has lateroventral setae on segments 2, 4, 6, 8 and 10. Regarding the ventral pattern of setae, males of *C. unangax* sp. nov. show ventromedial setae on segments 3 – 9, and females only have ventromedial setae on segments 2, 7 – 9. As for the discussed congeners, males of *C. abyssorum* have the same pattern as the new species, but females of *C. abyssorum* only have these setae on segments 2 and 9 (Adrianov & Maiorova, 2015); *C. cristatus* does not have ventromedial setae on segments 3 – 6 (only males are known, see Sánchez et al., 2013); males of *C. furugelmi* have ventromedial setae on segments 2 – 8, and females on segments 2 – 6 (Adrianov & Malakhov, 1999); specimens of *C. dordaidelosensis* lack these setae at least on segments 3 – 7 (only males are known, see Sørensen & Grzelak, 2018); and males of *C. glaurung* have paraventral setae on segments 3 – 9, while females have setae in ventromedial positions on segments 2, 7, and 8 and in paraventral positions on segments 3–6, and 9 (Sørensen & Grzelak, 2018). In addition, *C. unangax* sp. nov. shows ventrolateral setae on segment 1, a character absent in *C. abyssorum* (at least in females), *C. chukchiensis*, *C. cristatus*, *C. furugelmi*, *C. glaurung*, *C. dordaidelosensis* (see Higgins, 1991; Adrianov & Malakhov, 1999; Sánchez et al., 2013; Adrianov & Maiorova, 2015; Sørensen & Grzelak, 2018).

Based on the above characteristics, the males of *Cristaphyes abyssorum* seem to show many similarities with those of the new species. However, the number and arrangement of the setae of the dorsal series allow to unequivocally differentiate males of both species, since males of *C. abyssorum* have unpaired paradorsal setae on segments 2 – 4 and 7 – 9 (see Adrianov & Maiorova, 2015), a character absent in C. unangax sp. nov. Moreover, males of *C. abyssorum* have subdorsal/laterodorsal setae on segments 1 – 2 and 9 (see Adrianov & Maiorova, 2015), while males of the new species bear laterodorsal setae on segments 2, 4 and 8, plus paralateral ones on segments 1, 3, 5, 7 and 9.

Cristaphyes nubilis is the species that resembles the new species described herein most. As previously said, both have lateral terminal spines and a keel-shaped process on segment 10 surpassing the posterior margin of the trunk. Moreover, both species share the presence of middorsal process on all segments 1 – 10, cuticular extensions on segment 11, as well as the lateroventral seta pattern (Sánchez et al., 2014). Despite that only females of *C. nubilis* are known, the two species can be distinguished by the dorsal seta distribution, since *C. nubilis* has paradorsal setae on segment 1 and the remaining dorsal setae are lined up, all of them located in laterodorsal position (Sánchez et al., 2014). The former character is absent in *C. unangax* sp. nov.; and females of the new species lack dorsal setae on several segments (present only on segments 2 and 9), while males show alternating laterodorsal and paralateral setae, with the paralateral ones occurring on segments 1, 3, 5, 7 and 9, and the laterodorsal ones on segments 2, 4 and 8 (present also

on segments 6 and 9 in some specimens).

With regard to bathymetry, four deep-sea *Cristaphyes* species have been discovered so far. *Cristaphyes abyssorum*, *Cristaphyes fortis* Cepeda et al., 2019, *Cristaphyes microtubuliferus* Sørensen & Grzelak, 2024, and *C. nubilis* (see Sánchez et al., 2014; Adrianov & Maiorova, 2015; Cepeda et al., 2019; Sørensen & Grzelak, 2024). As discussed above, *C. abyssorum* and *C. nubilis* differ from the new species in several morphological characters. As for *C. fortis*, it was described from the Gulf of California, eastern Pacific Ocean, at 1440 – 1570 m depth, and it is easily distinguishable from *C. unangax* sp. nov. as *C. fortis* does not have a keel-shaped process on segment 10 surpassing the posterior margin of the trunk (see Cepeda et al., 2019). Finally, *C. microtubuliferus* was found from the continental rise of South Island, New Zealand, at 1002 – 1295 m depth. Similarly, this species can be distinguished from the new species described herein by the absence of a keel-shaped process on segment 10 that surpasses the posterior margin of segment 11 and by having very short lateral terminal spines (see Sørensen & Grzelak, 2024).

4.2. Diversity patterns and distribution of Kinorhyncha in the Aleutian Trench

Recent studies on Kinorhyncha from hadal environments have revealed that adult communities are more abundant compared to those found in abyssal environments (Grzelak et al., 2021; Sánchez et al., 2024). In addition, this research also showed that adult kinorhynchs did not follow a homogeneous distribution in hadal trenches, but their abundance was higher in the axis than on the slopes or terraces zone. Both findings on kinorhynch fauna were in line with the patterns observed for the general meiofaunal community (Danovaro et al., 2002; Jamieson et al., 2010; Schmidt & Martínez Arbizu, 2015; Leduc et al., 2016).

Our results show that the abundance of adult kinorhynchs remains relatively low along the bathymetric gradient studied (Fig. 5), from c.a. 3.500 to c.a. 7.200 m. However, two notable exceptions were observed, where their abundance reached striking maxima: one at a slope site located at 4.305 m depth (15 specimens, station 12) and another at an axis site at depths between 6.469 and 7.137 m (16 specimens, station 9). The high number of adult kinorhynchs found in another hadal site, located at 6.341 m, with 9 specimens (station 13), is also remarkable. The elevated abundance in the axis is congruent with patterns observed in other trenches. Grzelak et al. (2021) found a clear trend of increasing adult abundance with depth in the Atacama Trench, with the highest values recorded in the hadal zone. Regarding the South Orkney Trench, Sánchez et al. (2024) found a similar pattern when considering only adult specimens. The proliferation of animals along the trench axis may be due to the fact that, as hypothesised by other researchers, the axis acts as a reservoir of organic matter falling from the surface, enhancing the microbial activity (Wenzhöfer et al., 2016; Glud et al., 2021; Xu et al., 2021) that ultimately supports meiofaunal communities (Danovaro et al., 2003; Glud et al., 2013; Shimabukuro et al., 2022).

However, the elevated number of specimens found at one abyssal station is noteworthy (Fig. 5) (station 12: 15 adult specimens and 76 total kinorhynchs, considering both adults and juveniles). This finding may be attributed to the upwelling currents that occur around the Aleutian Islands, which provide additional nutrients to this specific region (Springer et al., 1996), or to the trench's orography. The south wall of the trench has a tilt of 4.5 – 6.0 %, whereas the north wall shows a much steeper slope with broad and relatively flat sediment-covered terraces (Jumars & Hessler, 1976; Brandt, 2022). Station 12 is located in the northern side of the trench, where terraces represent a common geographic feature. The presence of terraces facilitates the deposition and accumulation of food particles, thereby promoting the development of a thriving kinorhynch community.

In terms of species richness, the Kinorhyncha community of the hadal trenches has been shown to be dominated by a single species, named *E. mamaqucha* in the Atacama Trench (see Grzelak et al., 2021) and *E. australis* in the South Orkney Trench (see Sánchez et al., 2024). In fact, densities of these two species were higher at the hadal sites of their respective trenches. Similarly, in the Aleutian Trench, the hadal sites are dominated by a single species, *E. ultraabyssalis*, which is the only kinorhynch representative found at the deepest sites of the trench (from 6.469 to 7.237 m depth) (Fig. 5). This species was originally described by Adrianov & Maiorova (2019) from the Kuril-Kamchatka Trench. However, the original description did not include information on accompanying kinorhynch fauna, preventing direct comparisons of species richness or abundance patterns between the Kuril-Kamchatka Trench and the Aleutian Trench.

Our study also reveals the presence of 10 kinorhynch species in the Aleutian Trench, with many of them occurring in various regions of the North Pacific and Arctic Oceans. Two species originally described from the North-West Pacific have been found in the present study: *Condyloderes kurilensis*, described from the Kuril-Kamchatka Trench, and *Sphenoderes japonicus*, newly discovered from the Sea of Japan (see Adrianov & Maiorova, 2016, 2024). Another two species discovered from the Pacific, specifically from the Clarion-Clipperton Zone (CCZ, Tropical East Pacific) (see Sánchez et al., 2019, 2022), have been identified in our samples: *Cephalorhyncha polunga*, and *Echinoderes delaordeni*. Last, *E. hamiltonorum*, and *E. juliae*, described from the North Pacific (see Sørensen et al., 2018) are also present in the Aleutian Trench. It is worth mentioning that *C. kurilensis* and *E. juliae* were also reported from the CCZ (North Pacific) (Sánchez et al., 2022). Regarding the Arctic species, *E. angustus*, was discovered from the Disko Island and years later found at Spitsbergen, Arctic (see Higgins & Kristensen, 1988; Grzelak & Sørensen, 2018). Taking all this into account, it seems that the benthic deep-sea fauna of the North Pacific is capable of dispersing across the bathymetric barriers of the Aleutian Arc, that is, the Aleutian Trench and Aleutian Island Ridge. If so, several important implications can be inferred. Based on the shared fauna between the Aleutian and the Kuril-Kamchatka Trench, meiofauna of both regions may be interconnected through topographic features such as the Kuril Strait and/or the Commander Basing of the Bering Sea. Moreover, the Aleutian Trench may serve as a gateway for meiofaunal organisms migrating from the North Pacific to the Arctic. This is supported by the presence of several species found in the Bering Sea, within the trench itself, and further south, such as in the CCZ. The observed distribution of these species aligns with the main circulation patterns of the North Pacific, where the Alaskan Current and Alaskan Stream transport water masses from east to west, while the East Kamchatka Current flows southward from the Kamchatka Strait through the Kuril-Kamchatka Trench. These currents, particularly through the influence of the Western Subarctic Gyre, may play a role in shaping meiofaunal dispersal pathways (Budyansky et al., 2022; Andreev et al., 2020). Finally, kinorhynchs, along with other meiofaunal animals, may be passively transported by strong bottom currents of the trenches, which could function as dispersal corridors. This movement may follow either a longitudinal gradient (Grzelak et al., 2021) or a latitudinal gradient, depending on the alignment of the trench axis.

CRediT authorship contribution statement

Nuria Sánchez: Writing – review & editing, Writing – original draft, Visualization, Investigation, Funding acquisition, Data curation, Conceptualization. **Frederic Bonk:** Writing – review & editing, Resources, Methodology, Data curation. **Alberto González-Casarrubios:** Writing – review & editing, Writing – original draft, Investigation, Funding acquisition.

Declaration of competing interest

The authors declare that they have no known competing financial interests or personal relationships that could have appeared to influence

the work reported in this paper.

Acknowledgements

We would like to thank Prof. Dr. Pedro Martínez Arbizu who made the material from Aleut Bio (Aleutian Trench Biodiversity Studies, SO293) expedition (R/V Sonne) available for this study. We also wish to thank all the chief scientist of this expedition, Prof. Dr. Angelika Brandt, participants and the staff involved in this cruise and to the staff and students of the Senckenberg Research Institute, German Center of Marine Biodiversity Research (DZMB), Senckenberg am Meer, for helping in the process. The cruise was financed by the German Ministry of Education and Science (BMBF) as a contribution to the project (PTJ, grant number:03G0293A). AGC was supported by a predoctoral contract from the Community of Madrid (PIPF-2023). FB was supported by a predoctoral contract from SENCKENBERG Gesellschaft für Naturforschung (SGN). Taxonomic research made by AGC and NS were supported by the International Seabed Authority's Sustainable Seabed Knowledge Initiative: One Thousand Reasons Campaign (co-financed by the European Maritime and Fisheries Fund of the European Union, Project 101071214 — SSKI-I — EMFAF-2021-ISA-SSKI-IBA). We thank Dr. Birger Neuhaus, Dr. Martin V. Sørensen and an anonymous reviewer for their comments and suggestions, which have greatly improved the manuscript.

This is AleutBio publication # 19.

Data availability

Data will be made available on request.

References

Adrianov, A.V., Malakhov, V.V., 1999. Cephalorhyncha of the world ocean. KMK Scientific Press, Moscow, p. 328.

Adrianov, A.V., Maiorova, A.S., 2015. *Pycnophyes abyssorum* sp. n. (Kinorhyncha: Homalorhagida), the deepest kinorhynch species described so far. Deep-Sea Res. II: Top. Stud. Oceanogr. 111, 49–59. https://doi.org/10.1016/j.dsr2.2014.08.009.

Adrianov, A.V., Maiorova, A.S., 2016. *Condyloderes kurilensis* sp. nov. (Kinorhyncha: Cyclorhagida) — a new deep water species from the abyssal plain near the Kuril-Kamchatka Trench. Russ. J. Mar. Biol. 42 (1), 11–19. https://doi.org/10.1134/s1063074016010028.

Adrianov, A.V., Maiorova, A.S., 2019. *Echinoderes ultraabyssalis* sp. nov. from the Kuril-Kamchatka Trench – the first hadal representative of the Kinorhyncha (Kinorhyncha: Cyclorhagida). Prog. Oceanogr. 178, 102142. https://10.1016/j.pocean.2019.102142.

Adrianov, A.V., Maiorova, A.S., 2024. *Sphenoderes japonicus* sp. nov. – The first deep water representative of the family Semnoderidae (Kinorhyncha, Cyclorhagida) in the sea of Japan. Zool. Anz. 313, 161–174. https://doi.org/10.1016/j.jcz.2024.10.003.

Andreev, A.G., Budyansky, M.V., Khen, G.V., Uleysky, Y., 2020. Water dynamics in the western Bering Sea and its impact on chlorophyll a concentration. Ocean Dyn. 70, 593–602. https://doi.org/10.1007/s10236-020-01347-7.

Brandt, A. (2022). SO293 AleutBio (Aleutian Trench Biodiversity Studies) Cruise Report/Fahrtbericht, Cruise No. SO293, 24.07.2022 - 06.09.2022, Dutch Harbor (USA) - Vancouver (Canada). SONNE-Beritche; SO293; 1–209. doi: 10.48433/cr_so293.

Budyansky, M.V., Prants, S.V., Uleysky, M.Y., 2022. Odyssey of Aleutian eddies. Ocean Dyn. 1–22. https://doi.org/10.1007/s10236-022-01508-w.

Cepeda, D., Álvarez-Castillo, L., Hermoso-Salazar, M., Sánchez, N., Gómez, S., Pardos, F., 2019. Four new species of Kinorhyncha from the Gulf of California, eastern Pacific Ocean. Zool. Anz. 282, 140–160. https://doi.org/10.1016/j.jcz.2019.05.011.

Cepeda, D., Pardos, F., Zeppilli, D., Sánchez, N., 2020. Dragons of the deep sea: Kinorhyncha communities in a pockmark field at Mozambique Channel, with the description of three new species. Front. Mar. Sci. 7, 665. https://doi:10.3389/fmars.2020.00665.

Danovaro, R., Della Croce, N., Dell'Anno, A., Pusceddu, A., 2003. A depocenter of organic matter at 7800m depth in the SE Pacific Ocean. Deep-Sea Res. i: Oceanogr. Res. Pap. 50, 1411–1420. https://doi.org/10.1016/j.dsr.2003.07.001.

Danovaro, R., Gambi, C., Della Croce, N., 2002. Meiofauna hotspot in the Atacama Trench, eastern south Pacific Ocean. Deep-Sea Res. i: Oceanogr. Res. Pap. 49, 843–857. https://doi.org/10.1016/s0967-0637(01)00084-x.

Glover, A.G., Higgs, N., Horton, T. (2025). World Register of Deep-Sea species (WoRDSS). Accessed at https://www.marinespecies.org/deepsea on 2025-02-23. doi: 10.14284/352.

Glud, R.N., Berg, P., Thamdrup, B., Larsen, M., Stewart, H.A., Jamieson, J., et al., 2021. Hadal trenches are dynamic hotspots for early diagenesis in the deep sea. Commun. Earth Environ. 2, 21. https://doi.org/10.1038/s43247-020-00087-2.

Glud, R.N., Wenzhöfer, F., Middelboe, M., Oguri, K., Turnewitsch, R., Canfield, D.E., et al., 2013. High rates of microbial carbon turnover in sediments in the deepest oceanic trench on Earth. Nat. Geosci. 6, 284–288. https://doi.org/10.1038/ngeo1773.

González-Casarrubios, A., Cepeda, D., Pardos, F., Neuhaus, B., Yamasaki, H., Herranz, M., Grzelak, K., Maiorova, A., Adrianov, A., Dal Zotto, M., Di Domenico, M., Landers, S.C., Sánchez, N., 2023. Towards a standardisation of morphological measurements in the phylum Kinorhyncha. Zool. Anz. 302, 217–223. https://doi.org/10.1016/j.jcz.2022.11.015.

González-Casarrubios, A., Yamasaki, H. (2022). Kinorhyncha measurement database. Available from https://sites.google.com/a/meiobenthos.com/ laboratory/database/kinorhyncha-measurement-database (accessed 1 November 2024).

Grzelak, K., Sørensen, M.V., 2018. New species of *Echinoderes* (Kinorhyncha: Cyclorhagida) from Spitsbergen, with additional information about known Arctic species. Mar. Biol. Res. 14 (2), 113–147. https://doi.org/10.1080/17451000.2017.1367096.

Grzelak, K., Sørensen, M.V., 2019. Diversity and community structure of kinorhynchs around Svalbard: first insights into spatial patterns and environmental drivers. Zool. Anz. 282, 31–43. https://doi.org/10.1016/j.jcz.2019.05.009.

Grzelak, K., Zeppilli, D., Shimabukuro, M., Sørensen, M.V., 2021. Hadal mud dragons: first insight into the diversity of Kinorhyncha from the Atacama Trench. Front. Mar. Sci. 8, 670735. https://doi.org/10.3389/fmars.2021.670735.

Herranz, M., Stiller, J., Worsaae, K., Sørensen, M.V., 2022. Phylogenomic analyses of mud dragons (Kinorhyncha). Mol. Phylogenet. Evol. 168, 107375. https://doi.org/10.1016/j.ympev.2021.107375.

Higgins, R.P., 1991. *Pycnophyes chukchiensis*, a new homalorhagid kinorhynch from the Arctic Sea. Proc. Biol. Soc. Wash. 104 (1), 184–188. https://www.biodiversitylibrary.org/page/34808872.

Higgins, R.P., Kristensen, R.M., 1988. Kinorhyncha from Disko Island, west Greenland. Smithson. Contrib. Zool. 458, 1–56. https://doi.org/10.5479/si.00810282.458.

Jamieson, A.J., Fujii, T., Mayor, D.J., Solan, M., Priede, I.G., 2010. Hadal trenches: the ecology of the deepest places on Earth. Trends Ecol. Evol. 25, 190–197. https://doi.org/10.1016/j.tree.2009.09.009.

Jumars, P.A., Hessler, R.R., 1976. Hadal community structure: implications from the Aleutian Trench. J. Mar. Res. 34 (4), 547–560.

Leduc, D., Rowden, A.A., Glud, R.N., Wenzhöfer, F., Kitazato, H., Clark, M.R., 2016. Comparison between infaunal communities of the deep floor and edge of the Tonga Trench: possible effect of differences in organic matter supply. Deep-Sea Res. i: Oceanogr. Res. Pap. 116, 264–275. https://doi.org/10.1016/j.dsr.2015.11.003.

Lemenkova, P., 2021. Topography of the Aleutian Trench south-east off Bowers Ridge, Bering Sea, in the context of the geological development of North Pacific Ocean. Baltica. 34 (1), 27–46. https://doi.org/10.5200/baltica.2021.1.3.

Neuhaus, B., Blasche, T., 2006. *Fissuroderes*, a new genus of Kinorhyncha (Cyclorhagida) from the deep sea and continental shelf of New Zealand and from the continental shelf of Costa Rica. ZooL. Anz. 245, 19–52. https://doi.org/10.1016/j.jcz.2006.03.003.

Werner, R., Hoernle, K., Hauff, F., Portnyagin, M., Yogodzinski, G., Ziegler, A., eds. (2016). RV SONNE Fahrtbericht / Cruise Report SO249 BERING – Origin and Evolution of the Bering Sea: An Integrated Geochronological, Volcanological, Petrological and Geochemical Approach, Leg 1: Dutch Harbor (U.S.A.) - Petropavlovsk-Kamchatsky (Russia), 05.06.2016 - 15.07.2016, Leg 2: Petropavlovsk-Kamchatsky (Russia) - Tomakomai (Japan), 16.07.2016 - 14.08.2016. GEOMAR Report, N. Ser. 030. GEOMAR Helmholtz-Zentrum für Ozeanforschung, Kiel, Germany, 451 pp. doi: 10.3289/GEOMAR_REP_NS_30_2016.

Sánchez, N., García-Cobo, M., Shimabukuro, M., Zeppilli, D., Nomaki, H., González-Casarrubios, A., 2024. Discovery of a new Kinorhyncha species from the uncharted South Orkney Trench (Southern Ocean). Zool. Anz. 313, 315–331. https://doi.org/10.1016/j.jcz.2024.10.016.

Sánchez, N., González-Casarrubios, A., Cepeda, D., Khodami, S., Pardos, F., Vink, A., Martínez Arbizu, P., 2022. Diversity and distribution of Kinorhyncha in abyssal polymetallic nodule areas of the Clarion-Clipperton Fracture Zone and the Peru Basin, East Pacific Ocean, with the description of three new species and notes on their intraspecific variation. Mar. Biodivers. 52, 52. https://doi.org/10.1007/s12526-022- 01279-z.

Sánchez, N., Pardos, F., Martínez Arbizu, P., 2019. Deep-sea Kinorhyncha diversity of the polymetallic nodule fields at the Clarion-Clipperton Fracture Zone (CCZ). Zool. Anz. 282, 88–105. https://doi.org/10.1016/j.jcz.2019.05.007.

Sánchez, N., Pardos, F., Sørensen, M.V., 2014. Deep-sea Kinorhyncha: two new species from the Guinea Basin, with evaluation of an unusual male feature. Org. Divers. Evol. 14 (4), 349–361. https://doi.org/10.1007/s13127-014-0182-6.

Sánchez, N., Rho, H.S., Min, W.G., Kim, D., Sørensen, M.V., 2013. Four new species of *Pycnophyes* (Kinorhyncha: Homalorhagida) from Korea and the East China Sea. Sci. Mar. 77 (2), 353–380. https://doi.org/10.3989/scimar.03769.15a.

Sánchez, N., Yamasaki, H., Pardos, F., Sørensen, M.V., Martínez, A., 2016. Morphology disentangles the systematics of a ubiquitous but elusive meiofaunal group (Kinorhyncha: Pycnophyidae). Cladistics. 32 (5), 479–505. https://doi.org/10.1111/cla.12143.

Schmidt, C., Martínez Arbizu, P., 2015. Unexpectedly higher metazoan meiofauna abundance in the Kuril-Kamchatka trench compared to the adjacent abyssal plains. Deep Sea Res. II: Top. Stud. Oceanogr. 111, 60–75. https://doi.org/10.1016/j.dsr2.2014.08.019.

Shimabukuro, M., Zeppilli, D., Leduc, D., Wenzhöfer, F., Berg, P., Rowden, A.A., Glud, R.N., 2022. Intra-and inter-spatial variability of meiofauna in hadal trenches is linked to microbial activity and food availability. Sci. Rep. 12 (1), 4338. https://doi.org/10.1038/s41598-022-08088-1.

Springer, A.M., Piatt, J.F., Vliet, G.V., 1996. Sea birds as proxies of marine habitats and food webs in the western Aleutian Arc. Fish. Oceanogr. 5 (1), 45–55. https://doi.org/10.1111/j.1365-2419.1996.tb00016.x.

Sørensen, M.V., Dal Zotto, M., Rho, H.S., Herranz, M., Sánchez, N., Pardos, F., Yamasaki, H., 2015. Phylogeny of Kinorhyncha based on morphology and two molecular loci. PLoS One. 10 (7), e0133440. https://doi.org/10.1371/journal.pone.0133440.

Sørensen, M.V., Grzelak, K., 2018. New mud dragons from Svalbard: three new species of *Cristaphyes* and the first Arctic species of *Pycnophyes* (Kinorhyncha: Allomalorhagida: Pycnophyidae). PeerJ. 6 (e5653), 1–48. https://doi.org/10.7717/peerj.5653.

Sørensen, M.V., Grzelak, K., 2024. A new deep-sea *Cristaphyes* (Kinorhyncha: Allomalorhagida: Pycnophyidae) from the continental rise of South Island. New Zealand. n. z. J. Zool. 1–19. https://doi.org/10.1080/03014223.2024.2308020.

Sørensen, M.V., Rohal, M., Thistle, D., 2018. Deep-sea Echinoderidae (Kinorhyncha: Cyclorhagida) from the Northwest Pacific. Eur. J. Taxon. 456, 1–75. https://doi.org/10.5852/ejt.2018.456.

Wenzhöfer, F., Oguri, K., Middelboe, M., Turnewitsch, R., Toyofuku, T., Kitazato, H., et al., 2016. Benthic carbon mineralization in hadal trenches: assessment by in situ O_2 microprofile measurements. Deep-Sea Res. I: Oceanogr. Res. Pap. 116, 276–286. https://doi.org/10.1016/j.dsr.2016.08.013.

Xu, Y., Li, X., Luo, M., Xiao, W., Fang, J., Rashid, H., Peng, Y., Li, W., Wenzhöfer, F., Rowden, A.A., Glud, R.N., 2021. Distribution, source, and burial of sedimentary organic carbon in Kermadec and Atacama Trenches. J. Geophys. Res-Biogeo. 126 (5). https://doi.org/10.1029/2020JG006189.

Yamasaki, H., Neuhaus, B., George, K.H., 2018a. New species of *Echinoderes* (Kinorhyncha: Cyclorhagida) from Mediterranean seamounts and from the deep-sea floor in the Northeast Atlantic Ocean, including notes on two undescribed species. Zootaxa. 4387, 541–566. https://doi.org/10.11646/zootaxa.4387.3.8.

Yamasaki, H., Neuhaus, B., George, K.H., 2018b. Three new species of Echinoderidae (Kinorhyncha: Cyclorhagida) from two seamounts and the adjacent deep-sea floor in the Northeast Atlantic Ocean. Cah. Biol. Mar. 59 (1), 79–106. https://doi.org/10.21411/CBM.A.124081A9.

Yamasaki, H., Neuhaus, B., George, K.H., 2019. Echinoderid mud dragons (Cyclorhagida: Kinorhyncha) from Senghor Seamount (NE Atlantic Ocean) including general discussion of faunistic characters and distribution patterns of seamount kinorhynchs. Zool. Anz. 282, 64–87. https://doi.org/10.1016/j.jcz.2019.05.018.

Zelinka, C., 1896. Demonstration der Tafeln der Echinoderes-Monographie. Verh. Dtsch. Zool. Ges. 6, 197–199.

Zelinka, C., 1907. Zur Kenntnis Der Echinoderen. Zool. Anz. 32, 130–136.